

ZnS nanoparticles capped with watermelon rind extract and their potential application in dye degradation

R. Lakshmiathy^{1,4} · Mohan Kumar Kesarla^{2,3} ·
Anvesh Reddy Nimmala¹ · Srinivas Godavarthi² ·
Chandra Mohan Kukkambakam³ · Lorenzo Martinez Gomez² ·
N. C. Sarada¹

Received: 10 May 2016 / Accepted: 9 August 2016 / Published online: 23 August 2016
© Springer Science+Business Media Dordrecht 2016

Abstract We report fabrication of stable ZnS nanoparticles (NPs) using a green chemistry concept with watermelon rind extract as capping and stabilizing agent. The cubic structure of the NPs was evidenced by X-ray powder diffraction analysis and electron diffraction studies. Dynamic light scattering and high-resolution transmission electron microscopy studies revealed that the average size of the ZnS NPs was <12 nm. The bandgap of the ZnS nanocrystals was found to be 3.42 eV using ultraviolet–visible (UV–Vis) spectroscopy studies. The energy-dispersive X-ray spectrum of the fabricated ZnS NPs confirmed the elemental Zn and S signals without peaks from any impurities. The biomolecular capping of the ZnS NPs was analyzed using Fourier-transform infrared spectroscopy. An illustrative stabilization mechanism for the ZnS NPs is given using citrulline, a major phytochemical in watermelon rind extract. The obtained ZnS NPs showed good photocatalytic activity towards methylene blue dye degradation.

Keywords Zinc sulfide (ZnS) · Watermelon rind · Citrulline · Photocatalytic · Methylene blue

Electronic supplementary material The online version of this article (doi:[10.1007/s11164-016-2700-y](https://doi.org/10.1007/s11164-016-2700-y)) contains supplementary material, which is available to authorized users.

✉ N. C. Sarada
ncsarada@vit.ac.in

- ¹ Environmental and Analytical Chemistry Division, School of Advanced Sciences, VIT University, Vellore, Tamilnadu 632014, India
- ² Instituto de Ciencias Físicas, Universidad Nacional Autónoma de México, Avenida Universidad s/n, 62210 Cuernavaca, MOR, Mexico
- ³ Department of Chemistry, Madanapalle Institute of Technology and Science, Post Box No: 14, Kadiri Road, Angallu (V), Madanapalle, Chittoor District, Andhra Pradesh 517325, India
- ⁴ Centre for Material Science, KCG College of Technology, Karapakkam, Chennai, Tamilnadu 600097, India

Introduction

II–VI semiconductor NPs with wide bandgap have been studied due to their wide use in optoelectronics and catalytic applications [1]. Among II–VI semiconductor NPs, zinc sulfide (ZnS) is considered an important material due to its structural stability. In recent years, many methods have been developed to prepare semiconductor NPs using physical and chemical techniques. Physical methods such as liquid microwave irradiation [2], reverse micelles [3], chemical vapor deposition [4], solid–liquid chemical reactions under ultrasound [5], and hydrothermal techniques [6] have been used to synthesize ZnS NPs. All these methods utilize/require toxic chemicals, two or more process steps, and rigorous conditions such as low/high pressure, high temperature, etc. Synthesizing semiconductor NPs with uniform size, composition, and surface passivation is very important for any potential application. Furthermore, stabilizers prevent oxidation of semiconductor NPs to a greater extent and provide a dielectric barrier at the surface which partially prevents surface traps. In this regard, different passivating agents (capping ligands), such as sodium polyphosphate [7], chain thiols [8], long-chain alkyl phosphine [9, 10], and alkyl phosphine oxides [10], have been used to prevent uncontrollable growth of nanocrystals and self-aggregation. However, most such capping agents are toxic in nature. It is very important to note that organic stabilizers with functional groups make NPs soluble in different solvents and allow further handling.

Considering environmental safety issues, current research is increasingly focusing on green nanotechnological aspects. Simple, ecofriendly, economic methods to prepare ZnS NPs with desired phase control and well-defined morphology are required. The present paper focuses on green synthesis of ZnS nanocrystals using watermelon rind extract as capping agent. The presence of pectin, citrulline, cellulose, proteins, and carotenoids in watermelon rind was evidenced in earlier reports [11–13]. Earlier reports also clarify that watermelon rind aqueous extract is rich in citrulline, an α -amino acid which resembles a short-chain ligand with $-\text{COOH}$ group at one end and $-\text{NH}_2$ group at the other. The same was used previously for size-controlled synthesis of silver NPs [14]. Similarly, recent reports revealed successful synthesis of nitrogen-rich activated carbon [15] and gold NPs [16] using watermelon rind (WR) biomass. This work demonstrates synthesis of ZnS NPs of controlled size using phytochemicals of watermelon rind extract for capping, and their application for methylene blue dye degradation.

Experimental

Materials and reagents

The chemicals used for the synthesis of ZnS NPs were zinc acetate [$\text{Zn}(\text{OAc})_2$] and sodium sulfide (Na_2S). Methylene blue ($\text{C}_{16}\text{H}_{18}\text{N}_3\text{SCl}$) was selected to study the degradation efficiency of the ZnS NPs. All chemicals used were of analytical grade and obtained from Sigma-Aldrich.

Preparation of WR extract

Watermelon rind (WR) was obtained from a local fruit market and washed under tap water several times followed by double-distilled water. After thorough washing, WR was cut into small pieces and dried under sunlight for 7 days to remove all moisture content. Later, the dried WR pieces were washed with hot (70 °C) water to remove any soluble matter present and dried in an oven at 85 °C for 48 h. The oven-dried WR was powdered using a conventional mixer, then 1 g of this powder was added to 100 ml water and heated at 70 °C for 15 min and filtered with Whatman filter paper. The supernatant solution was used for fabrication of ZnS NPs.

Preparation of ZnS NPs

By mixing 1:1 molar ratio of zinc acetate and sodium sulfide (Na_2S) at room temperature, white precipitate of ZnS was observed. To this ZnS colloid, WR extract was added, followed by vigorous stirring using a magnetic stirrer for 90 min at room temperature then centrifugation at 10,000 rpm for 10 min. The product obtained after discarding the supernatant was dried in an oven at 100 °C for 1 h, then characterized to understand its optical and surface properties.

Characterization

Absorption spectrum

The absorption spectrum of the WR-capped ZnS was recorded using a JASCO V-670 double-beam spectrophotometer in the wavelength range of 200–800 nm.

X-ray powder diffraction (XRPD)

Powder XRD analysis of the synthesized ZnS NPs was carried out using a Bruker D8 Advance diffractometer (with Cu K_α radiation, $\lambda = 1.54 \text{ \AA}$) equipped with a Lynx eye detector and β -Ni filter, scanning in the 2θ range from 10° to 80° at 0.02°/min. The instrument was calibrated using lanthanum hexaboride (LaB_6) prior to analysis.

Fourier-transform infrared (FTIR) spectroscopy

FTIR measurements were carried out using a JASCO FT-IR 4100 instrument in diffuse reflectance mode with resolution of 4 cm^{-1} in KBr pellet. The FTIR spectrum of the ZnS NPs was recorded over the range from 4000 to 400 cm^{-1} .

Photoluminescence (PL) spectrum

The photoluminescence emission spectrum of the ZnS NPs was obtained using a Hitachi F7000 fluorescence spectrophotometer at excitation wavelength of 300 nm.

Dynamic light scattering

To determine the size distribution profile, the ZnS NPs were subjected to dynamic light scattering studies using a Beckman Coulter DelsaNano particle size analyzer.

Electron microscopy

To understand the size and morphology of the ZnS nanocrystals, a JEOL JEM 2100F high-resolution transmission electron microscope was used at operating voltage of 200 kV. The particles were well dispersed using an ultrasonicator and deposited on Cu grid with ultrathin holey-C film.

Photodegradation of methylene blue

Methylene blue (MB), a water-soluble dye, was tested for photodegradation by ZnS NPs. Dye degradation studies were carried out in the presence of UV light at 365 nm for a solution containing 30 mg ZnS nanopowder in 30 mL 50 ppm MB solution. From the reaction mixture, 2 mL of solution was withdrawn every 20 min to record UV–Vis absorption spectra. The absorbance of the MB samples at $\lambda_{\text{max}} = 665$ nm was noted from the spectra. The decrease in absorbance at λ_{max} for the dye after irradiation for definite time intervals gives the rate of decolorization and therefore the photodegradation efficiency of the NPs, calculated as

$$\%D = 100 \times [(A_0 - A_t)/A_0],$$

where t is the irradiation time of the sample, and A_0 and A_t are the initial absorbance and the absorbance at time t , respectively.

Results and discussion

To understand the performance of semiconductor nanocrystals, study of their optical absorption is important. UV–Vis absorption spectroscopy is an effective method to determine the bandgap of NPs. The UV–Vis spectrum of the synthesized ZnS nanoparticles is shown in Fig. 1; the calculated optical bandgap of the NPs was around 3.42 eV (Fig. 1b). This bandgap value is lower than the usual value of 3.68 eV for zincblende [17]. The optical bandgap energy and absorption edge greatly depend on the degree of structural disorder in the lattice [18]. This bandgap decrease can be ascribed to formation of localized electronic bandgaps within the forbidden gap due to local bond distortions and defects. A similar energy bandgap value was reported for zincblende by La Porta et al. [19].

One of the most important optical properties of the ZnS NPs is their photoluminescence (PL) emission, which depends on the size, shape, and surface energetic states, which are further influenced by surface passivation [20]. The PL spectrum of aqueous extract of watermelon rind showed no emission at the

excitation wavelength. The PL spectrum of the ZnS nanocrystals prepared in presence of citrulline-rich watermelon rind extract is presented in Fig. S1 (in the Supporting Information), showing two distinct bands around 340 and 400 nm. From literature, it can be noticed that the PL of uncapped ZnS NPs shows only a broad peak between 350 and 550 nm [21]. The strong emission peak at around 340 nm indicates the presence of dangling bonds of phytochemicals, especially citrulline, which resembles a short-chain anionic surfactant, with Zn^{2+} in the surface of the ZnS NPs [20]. This weak interaction between the dangling bonds of citrulline and point defects on the ZnS NP surface results in a reduced bandgap. The broad, low-intensity emission peak observed at 400 nm is due to S^{2-} vacancies on the surface [20].

XRPD analysis was carried out to determine the crystalline nature of the ZnS NPs mediated by WR extract. The diffraction peaks at 28.65° , 33.15° , 47.56° , 56.44° , 60.67° , and 76.99° correspond to (111), (200), (220), (311), (400), and (331) planes of cubic ZnS (Fig. 2). The typical broadening of the diffraction peaks is also observed, implying that the size of the ZnS NPs is very small. The lattice parameters are in good agreement with Joint Committee on Powder Diffraction Standards (JCPDS) card no. 03-065-0309, and no characteristic peaks of impurity phases are observed.

High-resolution transmission electron microscopy studies revealed that the size of the NPs was <12 nm. HRTEM images at various magnifications are shown in Fig. 3. Furthermore, their size was confirmed by the particle size analyzer, which found an average size of around 11.3 nm (see Fig. S2 of Supporting Information). The selected-area electron diffraction (SAED) pattern of the ZnS NPs showed concentric rings, indicating polycrystalline nature of the material. These fringes were indexed to (111), (220), and (311) planes of cubic ZnS phase with $d(111) = 3.11 \text{ \AA}$, $d(220) = 1.90 \text{ \AA}$, and $d(311) = 1.62 \text{ \AA}$, respectively, confirming the presence of cubic ZnS. These results are corroborated by the XRD pattern of the synthesized ZnS NPs.

The energy-dispersive X-ray spectrum of the ZnS NPs is shown in Fig. S3 (Supporting Information). The synthesized product showed clear signals of Zn and

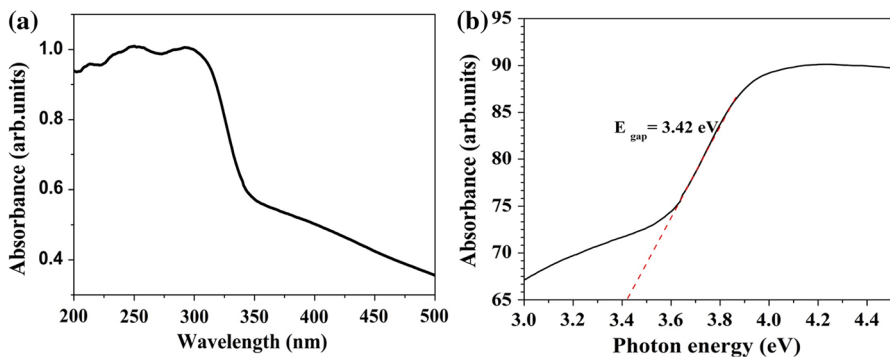


Fig. 1 UV-Vis spectrum of cubic ZnS nanostructure

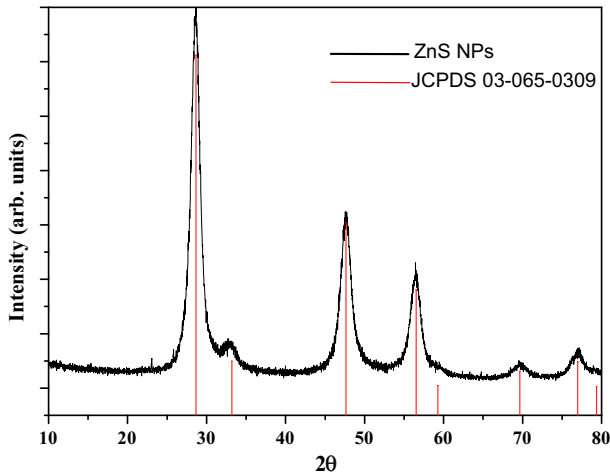


Fig. 2 XRPD pattern of synthesized ZnS nanoparticles

S. Other elemental signals including C are possibly due to biomolecules present within the WR.

The binding of biomolecules onto the ZnS surface was studied using FTIR spectroscopy, as shown in Fig. 4. The FTIR spectrum of WR-mediated ZnS NPs showed absorption peaks at 3441 cm^{-1} corresponding to O–H stretching, dual bands at 3419 cm^{-1} corresponding to N–H stretching, and a shoulder peak at 3200 cm^{-1} corresponding to an overtone of N–H bending vibration of primary amines. The peaks at 2926 and 2854 cm^{-1} are attributed to C–H stretching. The strong absorption peaks at 1631 cm^{-1} correspond to C–O stretching, and the band at 1568 cm^{-1} corresponds to N–H bending. C–C stretching was observed at 1402 cm^{-1} , whereas the absorption peaks at around 563 cm^{-1} correspond to Zn–S metal bond stretching. In earlier reports, for pure ZnS NPs without any capping, only peaks for Zn–S and a few moisture peaks could be observed [22, 23]. It is clear that biomolecular capping of ZnS NPs occurred, possibly due to binding of major phytochemical components of WR extract. For comparison, the FTIR spectrum of WR extract is shown in Fig. S4 (Supplementary Information).

From the FTIR and HRTEM analyses, it is clear that WR extract can bind to ZnS NPs and help to control their size. From the HPLC analysis of WR extract (see Fig. S5 of Supporting Information), citrulline was the major compound found, being expected to control the size of the ZnS nanocrystals as shown in Fig. 5. The major phytochemical citrulline contains carboxylic group at one end and primary amine at the other. This particular molecule has the ability to bind nanocrystals from both ends, i.e., carboxylic and amine group, through electrostatic interactions with the surface of ZnS nanoclusters. FTIR analysis supports these two types of binding onto the ZnS NPs. Colloids of ZnS nanocrystals obtained by this method were stable even after 6 months.

Prior to irradiation with UV light, ZnS NPs were submerged in MB dye solution for 30 min to ensure that adsorption had reached equilibrium, as the dye

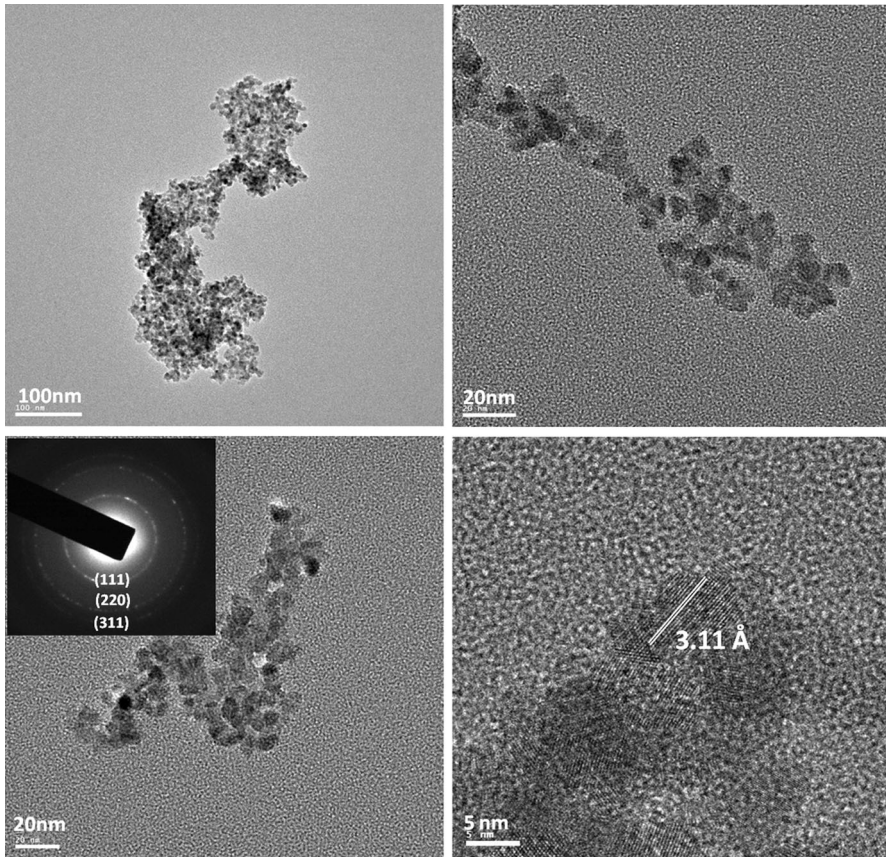


Fig. 3 HRTEM images of ZnS nanoparticles at various magnifications; inset shows SAED pattern of ZnS nanoparticles

concentration remained almost constant between 30 and 120 min (see Fig. S6 of Supplementary Information). Degradation of MB dye by ZnS NPs under UV light exposure for different time intervals is shown in Fig. 6. The results clearly show that the absorption maximum of MB dye at 665 nm gradually decreased with increasing irradiation time. No new absorption peaks appeared in the UV–Vis spectrum during the whole process. The percentage degradation of MB dye is plotted against irradiation time in the inset of Fig. 6. It can be seen from the recorded spectra that MB dye was degraded nearly 86 % in the presence of ZnS NPs within 180 min. These observations reveal that the synthesized ZnS NPs act as a good photocatalyst. This degradation is due to rapid formation of electron–hole pairs during photoexcitation of the ZnS NPs and the negative reduction potential associated with the excited electrons. This degradation capability is very high when compared with undoped pure ZnS reported in literature [24, 25]. From literature values, it is clear that pure ZnS NPs with size <10 nm showed only 63 % degradation of MB dye under UV irradiation for 300 min [24]. Similarly, Pourahmad [25] reported only

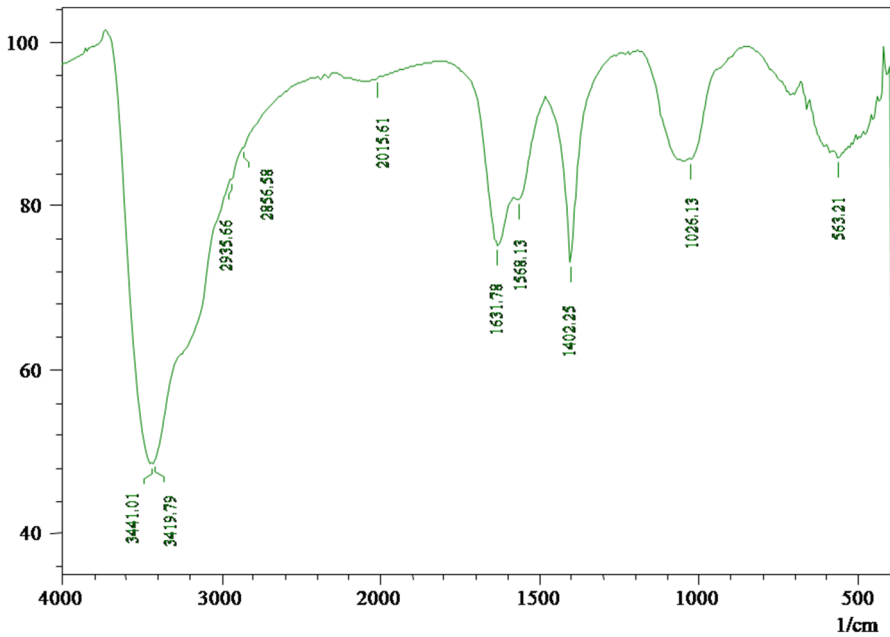


Fig. 4 FTIR spectrum of ZnS nanoparticles

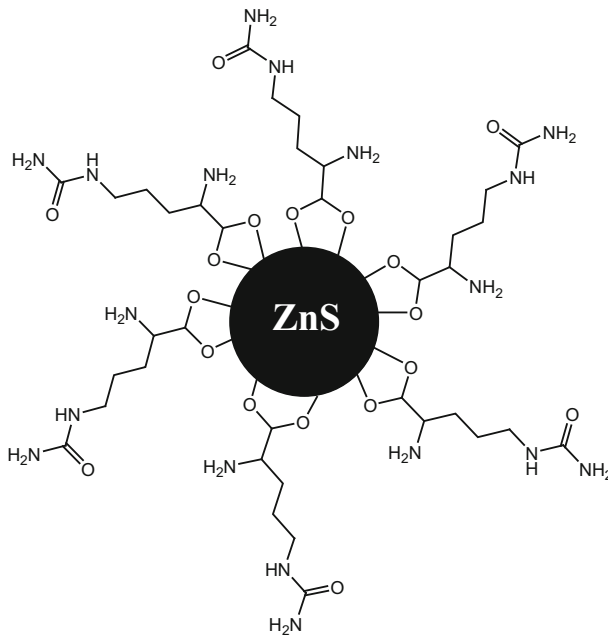


Fig. 5 Binding of citrulline on the surface of ZnS nanostructures

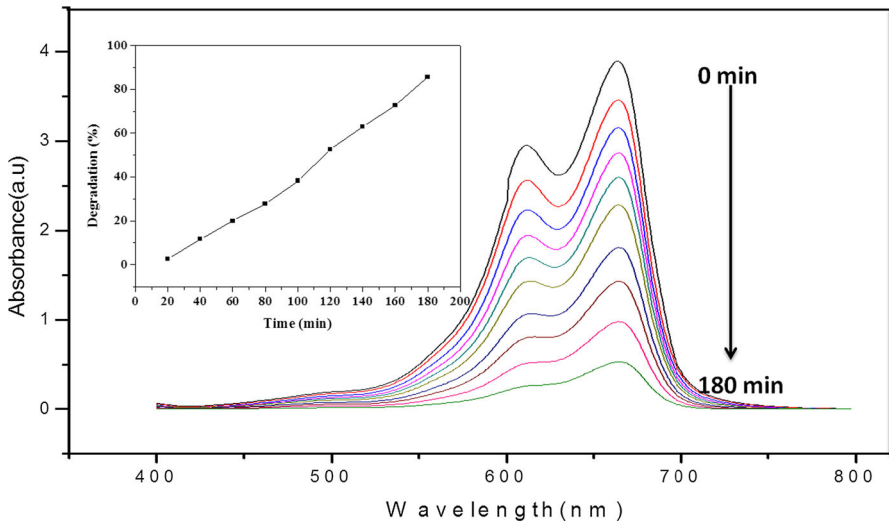
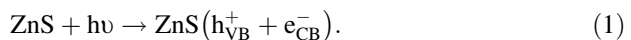


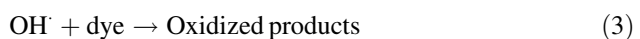
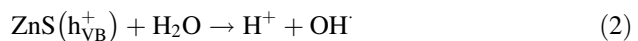
Fig. 6 MB dye degradation using ZnS nanoparticles; inset shows percentage degradation against time

45 % degradation after 20 min of irradiation with ZnS, with no further degradation being observed with increase in time. In the present study with WR-capped ZnS NPs, 86 % degradation of MB dye was achieved within 180 min. This enhanced degradation can be attributed to the biomolecular capping of the ZnS NPs. The reusability of the photocatalyst was tested by repeating the same experiment four times with the same catalyst. In each cycle, the catalyst was submerged in dye solution and subjected to UV irradiation. After 3 h, the absorbance of the dye solution was measured at 665 nm and the degradation percentage calculated. This recycling test for the ZnS photocatalyst showed 77 % degradation even after the fifth cycle (see Fig. S7 of Supplementary Information).

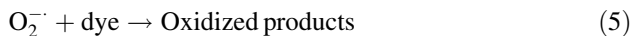
The complete mechanism for degradation of MB dye by the ZnS NPs is as follows: when irradiated with UV light, electrons from the valence band are excited to the conduction band, thus forming electron–hole pairs at the nanoparticle surface:



The formed hole has high oxidative potential and can directly oxidize the dye molecule into reactive intermediates. However, it is believed that hydroxyl radical formation is favored during decomposition of water by the hole, as shown in Eqs. (2) and (3).



On the other hand, the negative reduction potential associated with the conduction band converts molecular oxygen into superoxide radical, which in turns helps to degrade the organic dye compounds as shown in Eqs. (4) and (5).



The thus-formed superoxide radical and hydroxyl radical react drastically with dye molecules to oxidize them to water and carbon dioxide.

Moreover, the effective degradation of MB dye by the phytochemical-capped ZnS NPs is due to the fact that phytochemicals may serve as an effective host for dye adsorption, making electron transfer to dye molecules more feasible. Recent studies with capped NPs for dye degradation revealed that surface passivation of semiconducting NPs with amino acids and other aromatics resulted in formation of hydrophobic sites which could enhance the binding efficiency of MB dye onto the ZnS surface [26–28]. A similar phenomenon is possible in the present case, because the FTIR and HPLC analyses showed binding of citrulline and other molecules onto the ZnS NPs, in turn facilitating dye adsorption with simultaneous electron transfer, resulting in enhanced photocatalytic activity [29].

Conclusions

We report a simple, green method to fabricate and stabilize ZnS NPs. HRTEM analysis showed that the synthesized NPs were less than 12 nm in size. The NPs were stable for over 6 months, and the stabilization mechanism is illustrated using the major phytochemical in watermelon rind, i.e., citrulline. The obtained ZnS showed a bandgap of 3.42 eV, which is in agreement with other published literature for cubic zincblende. Thus, the synthesized ZnS NPs showed enhanced photocatalytic activity for degrading methylene blue dye.

Acknowledgments R.L. greatly acknowledges the help of VIT University, Vellore 632014, India for the platform provided to do this research. M.K.K. and S.G. are grateful for postdoctoral scholarships from Dirección General de Asuntos del Personal Académico - Universidad Nacional Autónoma de México (DGAPA-UNAM).

References

1. M. Khalkhali, Q. Liu, H. Zeng, H. Zhang, *Sci. Rep.* **5**, 14267 (2015)
2. J.J. Zhu, M. Zhou, J. Xu, X. Liao, *Mater. Lett.* **47**, 25 (2001)
3. P.S. Khiewa, S. Radimana, N.M. Huanga, S.Md Ahmed, K. Nadarajah, *Mater. Lett.* **59**, 989 (2005)
4. V. Bessergenev, E.N. Ivanova, YuA Kovalevskaya, S.A. Gromilov, V.N. Kirichenko, S.M. Zemskova, I.G. Vasilieva, B.M. Ayupov, N.L. Shwarz, *Mater. Res. Bull.* **30**, 1393 (1995)
5. Y.Y. She, J. Yang, K.Q. Qiu, *Trans. Nonferrous Metal Soc. China* **20**, s211 (2010)
6. J. Liu, J. Ma, Y. Liu, Z. Song, Y. Sun, J. Fang, Z. Liu, *J. Alloys Compd.* **486**, L40 (2009)
7. A.E. Raevskaya, A.L. Stroyuk, S.Y. Kuchmii, *Theor. Exp. Chem.* **39**, 158 (2003)
8. T. Vossmeier, L. Katsikas, M. Giersig, I.G. Popovic, K. Diesner, A. Chemseddine, A. Eychmuller, H. Weller, *J. Phys. Chem.* **98**, 7665 (1994)
9. Y. Kui, S. Singh, N. Patrino, V. Chu, *Langmuir* **20**, 11161 (2004)
10. C.B. Murray, D.J. Norris, M.G. Bawendi, *J. Am. Chem. Soc.* **115**, 8706 (1993)
11. A.M. Rimando, P.M. Perkins-Veazie, *J. Chromatogr. A* **1078**, 196 (2005)
12. R. Lakshminpathy, N.C. Sarada, *Int. J. Min. Process.* **122**, 63 (2013)

13. S.Y. Quek, N.K. Chok, P. Swedlund, *Chem. Eng. Process. Process. Intensif.* **46**, 386 (2007)
14. J.K. Patra, G. Das, K.H. Baek, *J. Photochem. Photobiol. B* **161**, 200 (2016)
15. R.J. Mo, Y. Zhao, M. Wu, H.M. Xiao, S. Kuga, Y. Huang, J.P. Li, S.Y. Fu, *RSC Adv.* **6**, 59333 (2016)
16. J.K. Patra, K.H. Baek, *Int. J. Nanomed.* **10**, 7253 (2015)
17. X. Fang, T. Zhai, U.K. Gautam, L. Li, L. Wu, Y. Bando, D. Golberg, *Prog. Mater. Sci.* **56**, 175 (2011)
18. F.A. La Porta, M.M. Ferrer, Y.V.B. Santana, C.W. Raubach, V.M. Longo, J.R. Sambrano, E. Longo, J. Andrés, M.S. Li, J.A. Varela, *J. Alloys Compd.* **556**, 153 (2013)
19. F.A. La Porta, J. Andrés, M.S. Li, J.R. Sambrano, J.A. Varela, E. Longo, *Phys. Chem. Chem. Phys.* **16**, 20127 (2014)
20. S.K. Mehta, S. Kumar, S. Chaudhary, K.K. Bhasin, *Nanoscale Res. Lett.* **4**, 1197 (2009)
21. S. Sapra, A. Prakash, A. Ghangrekar, N. Periasamy, D.D. Sarma, *J. Phys. Chem. B* **109**(5), 1663–1668 (2005)
22. K. Jeyasubramanian, M. Nisanthi, V.S. Benitha, N. Selvakumar, *Acta Metall. Sin. (Engl. Lett.)* **28**(1), 103 (2014)
23. R. Sahraei, G.M. Aval, A. Goudarzi, *J. Alloys Compd.* **466**, 488 (2008)
24. R. Chauhan, A. Kumar, R.P. Chaudhary, *J. Lumin.* **145**, 6 (2014)
25. A. Pourahmad, *Spectrochim. Acta A* **103**, 193 (2013)
26. A. Makhali, S. Sarkar, S.K. Pal, *Inorg. Chem.* **51**, 10203 (2012)
27. S. Baruah, S.S. Sinha, B. Ghosh, S.K. Pal, A.K. Raychaudhuri, J. Dutta, *J. Appl. Phys.* **105**, 074308 (2009)
28. N. Jain, A. Bhargava, J. Panwar, *Chem. Eng. J.* **243**, 549 (2014)
29. K. Mohan Kumar, S. Godavathi, E. Vázquez Vélez, M. Casales Díaz, M. Mahendhiran, A. Hernandez-Eligio, M. G. Syamala Rao L. Martinez Gomez, *J Sol–Gel. Sci. Technol.* (2016). doi:[10.1007/s10971-016-4136-7](https://doi.org/10.1007/s10971-016-4136-7)